NJC

Accepted Manuscript

This is an *Accepted Manuscript*, which has been through the Royal Society of Chemistry peer review process and has been accepted for publication.

Accepted Manuscripts are published online shortly after acceptance, before technical editing, formatting and proof reading. Using this free service, authors can make their results available to the community, in citable form, before we publish the edited article. We will replace this *Accepted Manuscript* with the edited and formatted *Advance Article* as soon as it is available.

You can find more information about *Accepted Manuscripts* in the Information for Authors.

Please note that technical editing may introduce minor changes to the text and/or graphics, which may alter content. The journal's standard Terms & Conditions and the Ethical guidelines still apply. In no event shall the Royal Society of Chemistry be held responsible for any errors or omissions in this *Accepted Manuscript* or any consequences arising from the use of any information it contains.

ROYAL SOCIETY OF CHEMISTRY

www.rsc.org/njc

The effect of vanadium substitution on photoluminescent properties of $KSrLa(PO_4)_x(VO4)_{2-x}$: Eu^{3+} phosphors: A new variant of phosphovanadates

Bal Govind Vats[a] *, Santosh K. Gupta[b] *, Meera Keskar[a], Rohan Phatak[a], S. Mukherjee[b] and S. Kannan[a]

[a]Fuel Chemistry Division, Bhabha Atomic Research Centre, Trombay, Mumbai-400085

[b]Radiochemistry Division, Bhabha Atomic Research Centre, Trombay, Mumbai-400085

*E-mail: bgvats@barc.gov.in; santufrnd@gmail.com

Abstract:

Eu^{3+} doped red emitting phosphors of formulae $KSrLa_{1-y}(PO_4)_x(VO4)_{2-x}$: yEu^{3+} (where x=0,1 and 2 and y = 0, 0.02, 0.05, 0.10 and 0.015) were synthesized by high temperature solid state reaction route. Compounds were characterized by powder XRD method and complete structure determination for $KSrLa(PO_4)(VO_4)$ were carried out by Rietveld refinement method. The compound is crystallized in rhombohedral system with space group ($R\bar{3}m$) .The structure of compound shows that La^{3+} is occupied at two positions namely trigonal antiprism (six cordinated) and truncated hexagonal bipyramidal (10 cordinated) with occupancy of 0.94 and 0.06, respectively. The effect of vanadium substitution on excitation and emission spectra of the compounds were investigated using time resolved photoluminescence spectroscopy (TRPLS). Lifetime of $^5D_0 \rightarrow {}^7F_2$ transition is determined for all the compounds which are in concordant with emission spectroscopic results. Judd-ofelt analysis of the compounds clearly shows that more polarized environment around Eu^{3+} in case of vanadate and phosphovanadate in comparison to phosphate leads to more colour purity of the emission, when excited by UV light.

1. Introduction:

Rare earth ions are mainly explored for their interesting physical properties like light emitting property due to their intra shell f-f transitions and magnetic property due to unpaired electrons in f-orbitals.[1] Among the rare earths, Eu^{3+} ion is an important activator which can emit fluorescence centred at about 612 nm (corresponding to $^5D_0 \rightarrow {}^7F_2$) when situated at noncentrosymmetric site.[2] Thus, materials doped with Eu^{3+} are being used for red emitting phosphor material.[3]. Moreover, the emission characteristics of Eu^{3+} ion is dependent upon the site at which Eu^{3+} is situated hence the emission can be used as a structure probe in the materials.[4]

Phosphates and vanadates are the most important host materials for obtaining the light emitting material via rare earth doping due to their thermal stability, low sintering temperature, chemical stability and environment friendly characteristics.[5] Many Eu^{3+} doped phosphates such as: $REPO_4$, $YBa_3(PO_4)_3$, $Ca_{10}Na(PO_4)_7$, $Ba_3La(PO_4)_3$, and $Ca_3(PO4)_2$ are used for materials for red emitting phosphor application.[6-10] Similarly many Eu^{3+} vanadates such as $NaCaLa(VO_4)_2$, $Ca_9Y(VO_4)_7$, $CsK_2Gd(VO_4)_2$, $REVO_4$, $Ca_3(VO_4)_2$ etc. are reported to have red emission.[11-15]

In all the reported materials Eu^{3+} ions is either having centrosymmetric or noncentrosymmetric sites. Depending on the site occupancy, colour purity of the emission is tuned in different materials. In noncentrosymmetric site, the induced electric dipoles ($^5D_0 \rightarrow {}^7F_2$) are more intense than the magnetic dipoles ($^5D_0 \rightarrow {}^7F_1$) hence contributing to high red colour purity which is desirable.[16] Due to above asymmetry condition for colour purity, many mixed phosphate system have been explored in recent years for red emitting phosphor material like $Ca_3(P_xV_{1-x}O_{4)2}$, $Y(P, V)O_4$, $(Ca_x Sr_{1-x})_3(PO_4)_3$, $K_2Bi(PO_4)(Mo,WO_4)$, $Ca_3Gd_7(SiO_4)_5(PO_4)O_2$ etc. to have enhancing effect on luminescence characteristic of Eu^{3+} ions.[17-21]

In $ABRE(PO_4)_2$ (where A = alkali metal, B = alkaline earth metal, RE = Rare earth or Y) system, many compounds like $NaCaLa(VO_4)_2$ [11] $KCaY(PO_4)_2$ [12] etc. having different structure types are reported in literature. For example, $KCaY(PO_4)_2$ is having hexagonal structure with space group $P6_222$ while $NaCaLa(VO_4)_2$ also crystallizes in rhombohedral system but space group is $R\bar{3}m$. In these systems no phosphovanadate is reported so far in literature. Hence, we report herein synthesis, structure and photoluminescence characteristic of $KSrLa(PO_4)_x(VO_4)_{2-x} : Eu^{3+}$ system. Europium is taken as a probe to see the changes in emission and lifetime on vanadate substitution. We have also tried to correlate these changes using Judd-Ofelt analyses.

2. Experimental:

2.1. Sample Preparation:

Single phase phosphors $KSrLa_{1-y}(PO_4)_x(VO_4)_{2-x} : yEu^{3+}$ (where x=0,1 and 2 and y = 0, 0.02, 0.05, 0.10 and 0.015) were prepared by conventional solid state route. The above series of phosphors were prepared from a mixture of KNO_3, $Sr(NO_3)_2$, $La(OH)_3$, Eu_2O_3, $NH_4H_2PO_4$ and NH_4VO_3 (all of which of AR grade) in appropriate stoichiometric ratio. The mixtures were first fired at 600°C for 10 hrs then temperature is raised to 950°C and kept for 24 hrs

with intermittent grinding. Final heating was done at 1050°C for 10 hrs to get the phase pure compound.

2.2. Sample Characterization:

Samples were characterized by powder X-ray Diffraction (XRD) Analysis (Rigaku Miniflex-600) with Cu Kα radiation (λ = 1.5406 A°) collected within the range 10° - 60° at 40kV and 15mA for phase identification. For Rietveld refinement, Data was collected within the range of 10°-100° with scan rate of 1°/min. Rietveld refinement was performed by Fullprof suite. [22] PL experiments were done on an Edinburgh CD-920 unit equipped with M 300 grating monochromators. The experimental data acquisition and analysis were done by F-900 software. A 150 W Xenon flash lamp having variable frequency range of 10–100 Hz was used as the excitation source. In present studies, all measurements were recorded with a lamp frequency of 100 Hz. Multiple Scans (at least five) were taken to minimize the fluctuations in peak intensity and maximize signal-noise ratio. Fluorescence lifetime measurements are based on well established Time-correlated single-photon counting (TCSPC) technique. Lifetime studies were done in the time range of 20 ms where the frequency of Xe lamp was fixed at 10 Hz. Approximately 25 mg of compound in powder form was mixed with few drops of 4 % collodion solution in amyl acetate and the resulting slurry was pasted over a glass plate using spatula. This was dried under room temperature and used for further studies.

3. Results and Discussion:

In $ABRE(PO_4)_2$ system(where A = alkali metal, B = alkaline earth metal, RE = Rare earth or Y) many compounds[11,12] are known but there is no report on the phosphovanadate mixed system in which phosphate groups are partly replaced by vanadate groups and hence compounds $KSrLa_{1-y}(PO_4)_x(VO_4)_{2-x} : yEu^{3+}$ (where x=0,1 and 2 and y = 0, 0.02, 0.05, 0.10 and 0.015) were synthesized by conventional solid state route. All the compounds obtained were white to light yellow in colour.

3.1 Phase purity and Crystal Structure: X-ray diffraction

The XRD patterns for $KSrLa(PO_4)_2$ (MLaP) , $KSrLa(PO_4)(VO_4)$ (MLaPV) and $KSrLa(VO_4)_2$ (MLaV) are shown in figure 1. As evident from the figure 1, the XRD patterns for the vanadate and phosphovanadate phase are shifted towards the lower 2θ values due to the large ionic radius of V^{5+} (0.355 A°) compared to P^{+5} (0.17 A°) in tetrahedral coordination.

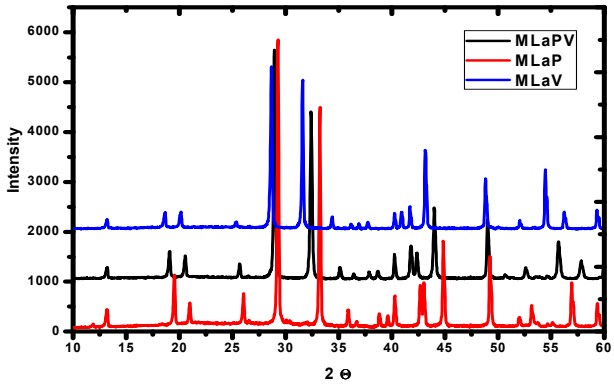

Figure 1: Powder XRD pattern of MLaP, MLaV and MLaPV phases

The XRD patterns match well with the reported phase $Sr_3(PO_4)_2$ (JCPDS No. – 24-1008). Compounds crystallize in rhombohedral system and all peaks are very well indexed with space group $R\bar{3}m$ (166). Structure refinement for $KSrLa(PO_4)(VO_4)$ was carried out by taking $Sr_3(PO_4)_2$ as a starting model. [23] In $Sr_3(PO_4)_2$ structure, Sr atom occupies two atomic positions corresponding to 3a and 6c Wyckoff positions which have six and ten co-ordinations respectively. Whereas in $KSrLa(PO_4)_2$ compound three atoms viz. K, Sr and La are distributed in 3a and 6c Wyckoff positions. Equal occupancy of these three atoms in the two sites gave bad fit to the XRD pattern and further refinement of occupancy parameters did not converge. Good starting crystal structure parameters are important for the convergence of the solution which is the underlying drawback of least square refinement used in Rietveld refinement programs. To overcome this problem, around ten thousand random occupancy distributions of K, Sr and La atoms over 3a and 6c Wyckoff positions were generated keeping the final stoichiometry of K:Sr:La as 1:1:1. These generated occupancies were used for calculating the structure factors and matched with observed structure factors. It was observed that, in all the good match cases (Sr/K) and La predominantly occupied 6c and 3a position respectively. Using this occupancy parameters further refinement of crystal structure was carried out. Figure 2 shows the observed, calculated and difference pattern of $KSrLa(PO_4)(VO_4)$ phase at room temperature. Details of crystallographic data are summarized in Table-1.

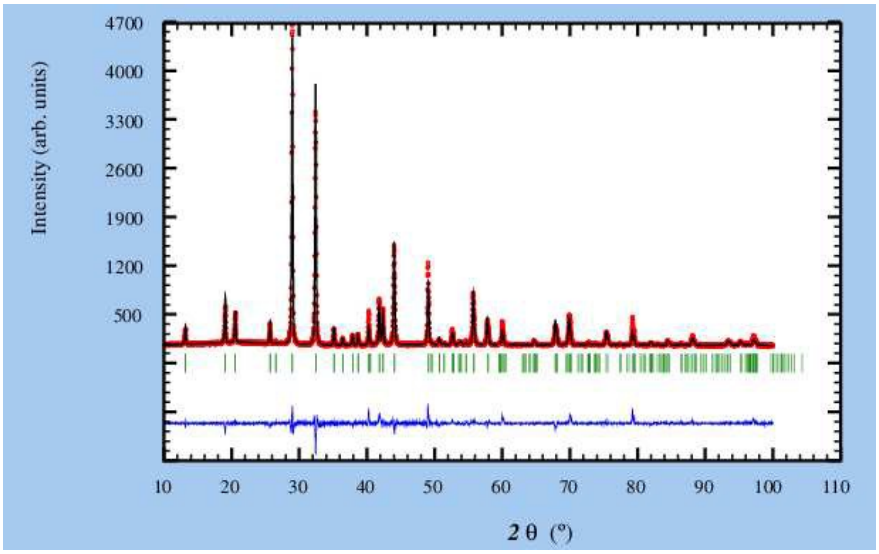

Figure 2: Observed (red), calculated (black) and difference pattern (blue) of $KSrLa(PO_4)(VO_4)$ phase at room temperature after rietveld refinement.

The structure of the compound contains phosphate and vanadate in tetrahedral coordination randomly distributed with 50% occupancy each and situated at C_{3v} site symmetry. At B site the occupancy of these three ions is (0.47K+0.5Sr+0.03La) and at A site the occupancy is (0.06 K + 0.94 La). It means 94% of La^{3+} ions are occupying 3a site, which has six coordinating oxygen atoms from phosphate/vanadate groups to form trigonal antiprism with D_{3d} symmetry and Wyckoff symbol *3a* and 6% La^{3+} ions are situated at B site to form a ten coordinated truncated hexagonal bipyramid with Wyckoff symbol 6c. Figure 3 shows unit cell view of MLaPV compound and coordination around A and B site.

Table-1: Rietveld refinement parameters for $KSrLa(PO_4)(VO_4)$

$KSrLa(PO_4)(VO_4)$	
Crystal System	rhombohedral
Space group	$R\bar{3}m$ (166)
Z	3
Cell parameters	a=b=5.5209 (1) ; c= 20.1449(6)
	α= 90°; β=90°; γ= 120°

Cell volume	531.754 (25)
χ^2	1.72
Rp	9.09
Rwp	11.8

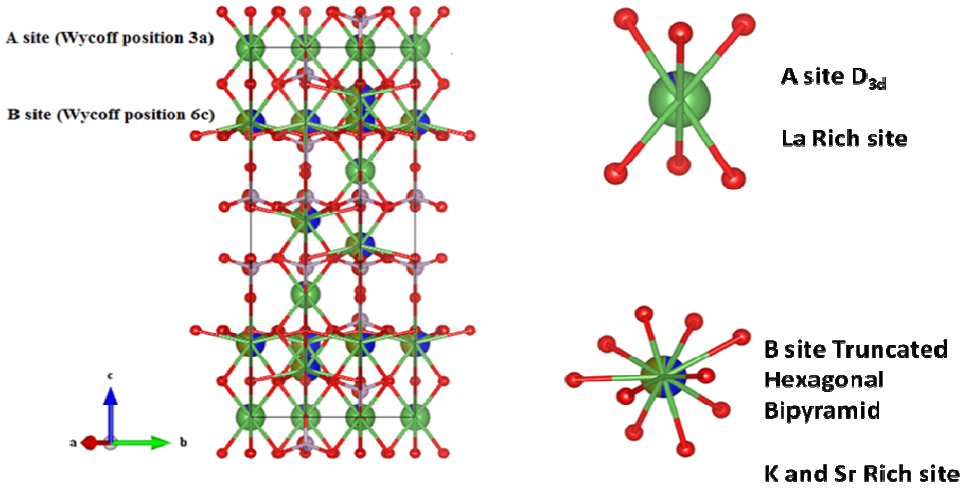

Figure 3: Unit cell view of crystal structure of MLaPV and coordination polyhedral view of A and B site

3.2. Photoluminescence properties of Eu^{3+} doped MLaP, MLaPV and MLaV

Figure 4 shows the excitation spectra of MLaP, MLaPV and MLaV doped with 2 mol% Eu monitored at 614 nm emission wavelengths. The excitation spectra comprise of a broad band between 220 -300 nm and narrow excitation peaks between 350 nm and 450 nm. The narrow weaker lines in the higher wavelength region (350–450 nm) are assigned to the intraconfigurational f-f transitions of the Eu^{3+} ions. Within these transitions, the ($^7F_0 \rightarrow {}^5L_6$) at 395 nm is the most intense ones and the less intense peaks were observed at 362 nm ($^7F_0 \rightarrow {}^5D_4$), 378 nm ($^7F_0 \rightarrow {}^5G_2$, $^5G_3$) and 415 nm ($^7F_0 \rightarrow {}^5D_3$). This indicates that the ultra-violet (UV), near-UV, UV B (UVB), and blue laser diodes/LEDs can act as effective pumping sources for the red emission from Eu^{3+} ions.

The interesting feature, observed in excitation spectra is a broad band between 220-300 which as referred as charge transfer band (CTB). In this process electron is transfer from the lower energy valence band (formed by filled 2p orbitals of oxygen atom) to a lower valence

intermediate states (a $4f^7$ Eu^{2+} state-formed due to transfer of oxygen 2p electron to Eu^{3+}). It is reported that the position of CTB is affected by various factors viz. ionic size, covalency, coordination number, polarizability, electronegativity etc **[24, 25]**.

Position of CTB is related to environmental factor (h_e) through an empirical relation formulated by Li et al **[26]**.

$$\mathbf{E_{CTB} = A+B\ exp\ (-kh_e)} \qquad \mathbf{(1)}$$

where A, B and k are parameter solely dependent on nature of lanthanide ion.

It is observed at 252 nm in case of pure phosphate MLaP: Eu^{3+}; but red shifted to around 274 nm when vanadate is introduced.The difference in CTB of phosphate and phosphovanadate is due to difference in position of valence band w.r.t to intermediate state which is $4f^7$ ($O^{2-} \rightarrow Eu^{3+}$) in case of phosphate and $3d^1$ in case of phosphovanadates ($O^{2-} \rightarrow V^{5+}$) **[24]**. Vanadium introduction has two prominent effect; (i) since P-O bond is more stable than V-O; oxygen that takes part in the formation of VB or conduction band (CB) lies at higher energy in presence of vanadium and (ii) introduction of vanadium also increases the covalency and thereby it causes larger splitting of Eu^{3+} 5d states (which forms VB or CB) and hence first 5d states will be at lower energy **[24]**.

Thus overall energy difference between VB and intermediate state decreases in presence of vanadium. Therefore, it could be easier for the electronic transition from the 2p orbital of O^{2-} to the 4f orbital of Eu^{3+} in MLaV or MLaPV host than that in MLaP and thus the CTB energy of Eu^{3+} is less and peak is correspondingly red shifted. Moreover, width of CTB is more in MLaV and MLaPV than MLaP as shown in the **Figure 4**. It is reported that V- O charge transfer occurs around 310 nm **[11]** so overlapping of V – O and Eu – O band may give rise to broader CTB as compared to that of MLaP.

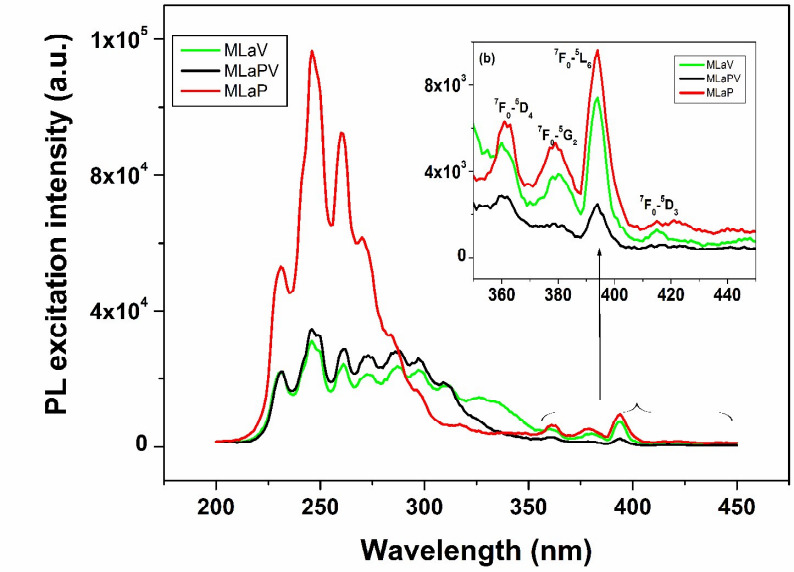

Figure 4: Excitation spectrum of MLaP, MLaPV and MLaV doped with Eu^{3+} (2.0 mol %) under emission corresponding to $^5D_0$-$^7F_2$ transition (614 nm). Inset shows the magnified image of intra f—f transition of europium.

Figure 5 shows the emission spectra of 2.0 mol % Eu^{3+} doped MLaP, MLaPV and MLaV under excitation of 274 nm corresponding to oxygen to europium CTB. The emission spectrum for all the three samples exclusively contains very strong bands of $^5D_0 \rightarrow {}^7F_1$ (592 nm), $^5D_0 \rightarrow {}^7F_2$ (614 nm), $^5D_0 \rightarrow {}^7F_3$ (653 nm) and $^5D_0 \rightarrow {}^7F_4$ (704 nm) and relative weaker emission at 579 nm corresponding to $^5D_0 \rightarrow {}^7F_0$.

$^5D_0 \rightarrow {}^7F_1$ emission of Eu^{3+} ion at 592 nm is of magnetic dipole origin (referred as magnetic dipole transition MDT) and its intensity is mostly unaffected by local chemical environment around the Eu^{3+} ion, whereas the $^5D_0 \rightarrow {}^7F_2$ emission of Eu^{3+} ion at 614 nm is hypersensitive electric dipole transition, EDT which means that its intensity is much more affected by the local symmetry/environment around the Eu^{3+} ion and the nature of the ligands compared to other ED transitions.

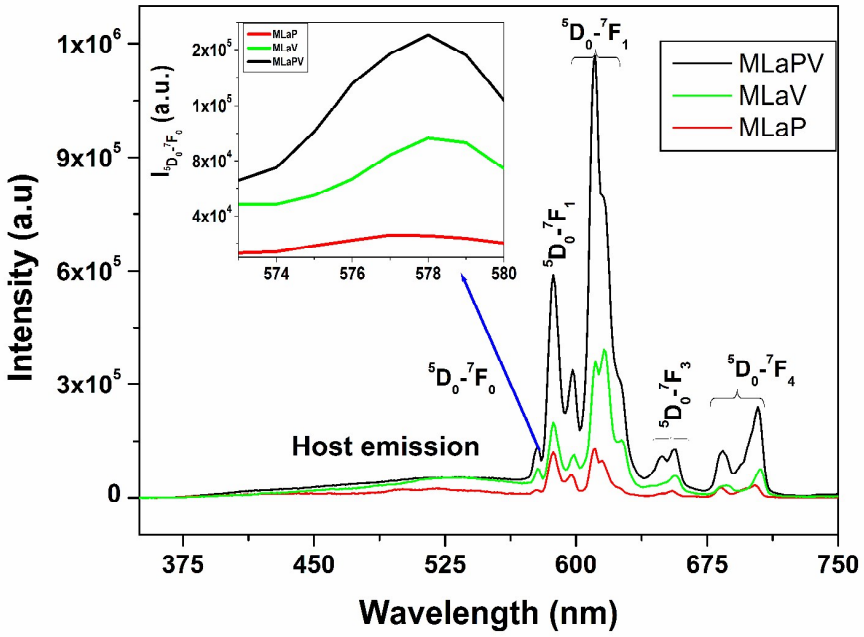

Figure 5: Emission spectrum of MLaP, MLaPV and MLaV doped with Eu^{3+} 2mol% under excitation of 274 nm. Inset in the figure show magnified image of $^5D_0$-$^7F_0$ emission line.

The integral ratio of EDT and MDT emission intensity, which is known as asymmetry ratio (R), gives various structure related information but alone it cannot be used as a measure of the asymmetry of the coordination environment around Eu^{3+}. It indeed is a function of various factors such as structure of the coordinating polyhedra, nature of ligand (polarizability) and not only the symmetry of the Eu^{3+} site **[27]**.

Although point group symmetry around La^{3+} site is D_{3d} which is expected to have centre of inversion and therefore emission characteristics around europium which is expected to occupy La^{3+} ion at D_{3d} site should reflect this i.e. low intensity of $^5D_0 \rightarrow {}^7F_2$, absence of $^5D_0 \rightarrow {}^7F_0$ transition **[28]** and fewer stark component due to stark splitting pattern **[27]**. But in this case emission spectra of all three sample shows intense $^5D_0 \rightarrow {}^7F_2$, presence of forbidden $^5D_0 \rightarrow {}^7F_0$ transition and considerable large extent of crystal filed splitting.To see if any changes in the emission characteristics of Eu^{3+} at low temperature we have performed PL measurements at 77 K. The emission spectra of MLaP:Eu and MLaPV:Eu at 77 K and 300 K under similar settings under cryostat is shown as supplementary data **(ESI, † Fig. S1 and S2 respectively)**. A low temperature experiment doesn't give any light on this except the enhancement in emission intensity and decay time along with peak narrowing and resolution of some fine structure in $^5D_0$-$^7F_3$ transition.

To probe the reason behind it we have also carried out lifetime measurements corresponding to the $^5D_0$ level of Eu^{3+} ions in MLaP, MLaPV and MLaV doped with Eu^{3+} has been carried out and shown in **Figure 6** at excitation wavelengths of 252 nm (for MLaP) and 274 nm (for MLaV/MLaPV) monitoring emission at 611 nm on a 40 ms scale. All the profiles are fitted using monoexponential decay:

$$\mathbf{I = I_0 exp\ (-t/\tau)} \qquad \mathbf{(1)}$$

Where *t* is the times of measurement and τ are the decay time values.

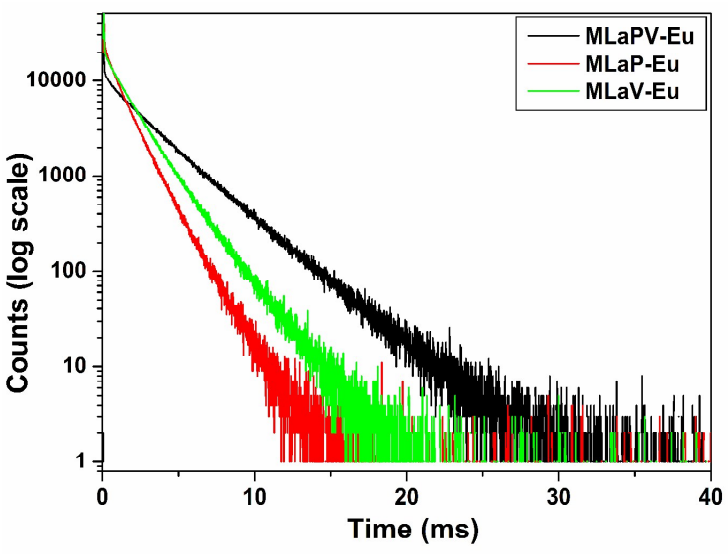

Figure 6: Luminescence decay time profile of MLaP, MLaPV and MLaV doped with Eu^{3+} (λ_{ex}- CTB and λ_{em} – 611 nm)

The presence of single lifetime is not necessarily related to Eu^{3+} occupying single site (homogenous environment around Eu^{3+}) because it is possible that two different site with similar lifetime values or intra-site energy transfer can give rise to pseudo-first order behaviour. If this is the case Eu^{3+} may be occupying both La^{3+} as well as Sr^{2+} site though majority will occupy La^{3+} site (because of charge and size consideration). Now there are three factors which lower the symmetry around Eu^{3+} and indeed it is not exactly D_{3d} (i) size mismatch between Eu^{3+} and La^{3+}/Sr^{2+} and (ii) charge mismatch between Eu^{3+} and Sr^{2+}. The overall lowering of symmetry get's reflected in origin of $^5D_0$-$^7F_2$ and $^5D_0$-$^7F_0$ and more stark components (large crystal filed splitting).

The life time values are 3.05, 1.812 and 1.261 ms respectively for Eu^{3+} doped MLaPV, MLaV and MLaP.

It is quite interesting to observe that for MLaPV: Eu^{3+} and MLaV: Eu^{3+} the integral intensity of EDT is much higher than that of MDT with respective asymmetry ratio of values of 2.46

and 3.21 while in MLaP:Eu the asymmetric ratio is closer to 1.0(~1.17). The same can be understood form the view that oxygens from vanadate groups are more polarisable with respect to phosphate group due to large electronegativity difference between vanadium and phosphorus. This more polarisable environment around Eu^{3+} causes more distortion around it giving rise to more intense EDT transition ($^5D_0 \rightarrow {}^7F_2$) in vanadate and phosphovanadate in comparison to phosphate. Such observation was also observed in case of $(Y_{0.95}Eu_{0.05})(V_{1-z}P_z)O_4$; where Wu *et al.* had observed decrease in R/O ratio as the P/V (phosphate to vanadate) ratio is increase i.e. more and more phosphate is incorporated **[29]**. At this point we can say the local distortion around europium ion in MLaP is smaller than that in MLaPV and MLaV because of low polarizability of phosphate group compared to vanadate.

The fact that MDT (orange emission) is equally intense as EDT (red emission) in MLaP:Eu^{3+}; it can't served as good red phosphor because spectral color purity required for red emission in white LEDs will be of poorer quality.

It is also reported that in case of individual vanadate system; host to Eu^{3+} energy transfer (ET) is more efficient than in phosphate based phosphor. This is because of the fact in vanadate system ET to europium goes via vanadate ion whereas in case of phosphate ET to europium proceeds without going to phosphate **[30]**. This is the probable reason why in case of phosphate host; europium emission intensity is comparatively less compared to vanadate.

But interestingly although asymmetry ratio is higher for MLaV: Eu^{3+} due to highest polarizing environment but emission intensity is higher for mixed compound i.e. MLaPV:Eu^{3+}. Similar results we have also observed in case of mixed tungstate and molybdate compound of thorium; where also maximum luminescence output is not observed in individual molybdate or tungstate but in mixed molybdate-tungstate $ThMo_{1.5}W0_{.5}O_8$ doped with europium ion **[31]**. Higher emission intensity in MLaPV:Eu^{3+} may be because of the two facts. One is that in mixed phosphovanadate presence of phosphate ion restricts the energy transfer among vanadate ions itself and passes on the energy from host to europium ion more efficiently and other one is because of more assymetry around the Eu^{3+} site in MLaPV:Eu^{3+} because of 50% replacement of phosphate by vanadate groups. The maximum emission output of MLaPV sample is also confirmed by performing low temperature measurement **((ESI, † Fig. S2)**

3.3. Judd-ofelt analysis of Eu^{3+} ion doped MLaP, MLaPV and MLaV

Judd-ofelt analysis is a very powerful tool for evaluating photophysical properties of europium ion in doped sample using the corrected emission spectrum. The details of all the calculations used are explained extensively elsewhere **[31, 32]**. For all the calculation corrected spectra corresponding to CTB excitation wavelength is used.

The value of refractive index used for MLaP, MLaPV and MLaV is 1.65, 1.86 and 2.07 respectively calculated using Gladstone Dale equations

$$\frac{n-1}{\rho} = k1\frac{p1}{100} + k2\frac{p2}{100} + k3\frac{p3}{100} + k4\frac{p4}{100} + k5\frac{p5}{100} \quad \textbf{(2)}$$

Where k = Gladstone-Dale constant (n-1/ρ) of chemical species i, p= percentage of chemical species. Data used in the calculation of refractive index for MLaP, MLaPV and MLaV is mentioned in **Table 2**. Density of MLaP, MLaPV and MLaV used is 4.478, 4.455 and 4.432 g/cc respectively.

Table 2: Data used in calculation of refractive index for MLaP, MLaPV and MLaV

	Density (g/cc)	Refractive index
K_2O	2.35	1.50
SrO	4.70	1.99
La_2O_3	6.51	2.14
P_2O_5	2.39	1.60
V_2O_5	3.36	2.30

It is well known that the JO parameter Ω_2, is an indication of the covalent character and structural changes in the local environment around Eu^{3+} ion (short range effects), while Ω_4 intensity parameters are long range parameters that can be related to the bulk properties such as viscosity and rigidity of the inorganic matrices.. Judd Ofelt parameter and other photophysical properties for Eu^{3+} doped MLaPV, MLaV and MLaP are listed in **Table 3**. It can be very well seen from the **Table 3** that Ω_2 values are higher in MLaV (2.05) and MLaPV (2.14) in comparison to MLaP (1.76). This trend indicates the more covalency in Eu-O bond as well as more distortion around Eu^{3+}as vanadate is incorporated in place of phosphate in the matrix. Higher value of Ω_4 in MLaP signifies more rigid structure in phosphate compared to vanadate systems. The other interesting observation is that Ω_4 value is greater than Ω_2 in MLaP indicating the whereas Ω_2 value is greater than Ω_4 in case of MLaV and MLaPV indicating the existence of asymmetric environment around europium ion.existence of relative symmetric environment with inversion centre around Eu^{3+} ion in MLaP.

The calculated τ_R for the excited $^5D_0$ level of Eu^{3+} ion in all the three sample was found to be larger than the τ_{exp}. This difference in τ_{exp} and τ_R can be attributed to decay by nonradiative pathways. There are lots of factor which contributes to non-radiative transition such as presence of surface defects, low vibrating oscillator (OH, CO, CO_2 etc), inhomogeneous surface etc. τ_{NRAD} for MLaPV is highest means that decay rate through nonradiative pathway is less efficient in MLaPV in comparison to MLaV and MLaP which gives rise to highest quantum yield for MLaPV.

Table 3: J-O intensity parameters and radiative properties for Eu^{3+} doped, MLaP, MLaPV and MLaV

PL	MLaPV: Eu^{3+}	MLaV: Eu^{3+}	MLaP: Eu^{3+}
τ_{exp}(ms)	3.05	1.81	1.26
τ_{RAD} (ms)	5.53	4.03	3.63
τ_{NRAD} (ms)	6.82	3.29	1.93
η(%)	55.2	45.0	34.7
I_{02}/I_{01}	2.46	3.21	1.17
$\Omega_2(*10^{-20}\,cm^2)$	2.14	2.05	1.76
$\Omega_4(*10^{-20}\,cm^2)$	1.97	1.23	2.62

3.4. Effect of Concentration variation on PL properties of europium in MLaPV:

Figure 7a and 7b shows the effect of concentration on PL emission intensity and lifetime. It was observed that, the emission intensity of europium ion increases initially with the increase in concentration, reaching maxima at 10.0 mol % and beyond that it reduces substantially. This phenomenon is attributed to concentration quenching. In terms of intrinsic quantum efficiency also trends remains the same wherein 10.0 mol % precedes over other with highest η value of 67.8 % whereas 2.0 mol % is having the lowest value with 55.2 %. On the other hand quantum efficiency value for 5.0 and 15.0 mol % is 59.4 and 62.3 %. Thus the optimum concentration i.e. one which is giving maximum output in MLaPV:Eu is 10.0 mol % doped sample. The concentration quenching leading to decrease in emission intensity

beyond certain concentration is due to energy transfer from one europium ion to another europium ion non-radiatively. Based on the minimum distance require for non-radiative energy transfer known as critical distance; one can explain the mechanism of concentration quenching. Generally in doped system; non-radiative energy transfer takes place via two different mechanisms (i) Forster resonance energy transfer (FRET or multipolar interaction) and (ii) Dexter mechanism (exchange overlap).

Fluorescence resonance energy transfer (FRET) is a distance-dependent interaction between the electronic excited states of two fluorophore (same or different) in which excitation energy is transferred from a donor molecule (D) to an acceptor molecule (A) non-radiatively. The efficiency of FRET is dependent on the inverse sixth power of the intermolecular separation ($1/\boldsymbol{R}^6$).

Primary Conditions for FRET:

1. D and A must be in close proximity (typically 10–100 Å).
2. The absorption spectrum of the A must overlap the fluorescence emission spectrum of the D (Figure 1).
3. D and A transition dipole orientations must be approximately parallel.

On the other hand Dexter mechanism (also known as exchange or coalitional energy transfer) is another dynamic quenching mechanism. It involves a overlap of orbital and is a short-range phenomenon (≤ 10 Å) that decreases with $e^{-\boldsymbol{R}}$ and depends on spatial overlap of D and quencher molecular orbital's.

Considering the geometrical features in host; one can roughly calculate critical transfer distance (R_c) for non-radiative energy transfer using the relation given by Blasse **[33]**.

$$\boldsymbol{R_C = 2\left(\frac{3V}{4\pi N X_C}\right)^{\frac{1}{3}}} \qquad \textbf{(3)}$$

Here V is the volume of the unit cell, X_C the critical concentration and N the number of available crystallographic sites occupied by the activator ions in the unit cell. Values of V and N for the crystalline MLaPV 531.749 $Å^3$ and 3 (number of lanthanum ion in one unit cell) respectively. Considering X_C =10.0 % (0.1), critical energy transfer distance R_c in MLaPV: Eu was calculated to be 41.13 Å. In this case, the Eu^{3+}- Eu^{3+} distance is much larger than 10 Å. Thus the possibility of concentration quenching by Dexter mechanism is ruled out. Therefore, the electric multipolar interaction is responsible for the energy transfer among the Eu^{3+} ions in MLaPV.

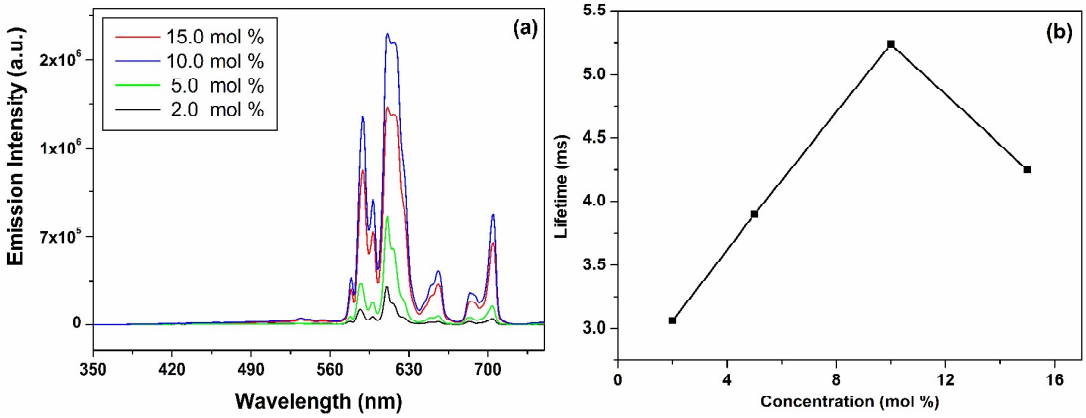

Figure 7: Effect of concentration on (a) PL emission spectrum (λ_{ex}-274 nm) and (b) Lifetime values of europium in MLaPV.

To evaluate the material performance on color luminescent emission, CIE chromaticity coordinates were evaluated for MLaPV, MLaV and MLaP Eu doped phosphors under CTB excitation. It can be clearly seen from the **Figure 8** and the calculated values, that MLaPV: Eu sample give an in intense red emission due to presence of relatively intense 614 nm lines ($^5D_0 \rightarrow {}^7F_2$) under 352 nm excitation. It was also observed from the respective emission spectrum that intensity of red line corresponding to $^5D_0$–$^7F_2$ transition of europium is maximum in MLaPV:Eu^{3+} compared to MLaV and MLaP which is also getting reflected in its high red color index and can be a potential phosphor to be used in White LEDs.

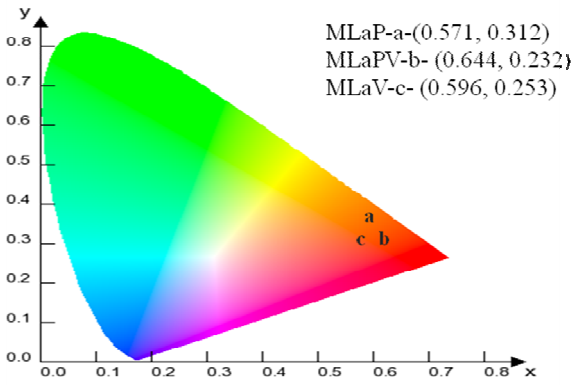

Figure 8: CIE diagram showing the co-ordinates and representing the color emitted by MLaP, MLaV and MLaPV doped with Eu^{3+} on CTB excitation

4. Conclusion:

Phase pure Eu^{3+} doped $KSrLa(PO_4)_x(VO4)_{2-x}$ where x=0,1 and 2 compounds were synthesizes by solid state reaction route. All the compounds were crystallized in

Rhombohedral lattice with $R\bar{3}m$ (166) space group. Rietveld refinement for MLaPV shows two metal sites A and B where most of the La^{3+} (94%) was situated at 3a Wyckoff position while K(100%) and Sr (94%) was situated at 6c Wyckoff position. Excitation spectra of the compounds show that as vanadate is doped in phosphate the CTB band becomes broad and red shifted to the higher wavelength as a result of vanadate substitution because of two reasons: 1. Due to lower energy gap of VB and intermediate state ($4f^7$ Eu^{2+}) after vanadium substitution 2. Due to mixing of Eu-O and V-O charge transfer bands. Emission spectra of the Eu^{3+} doped compounds show that asymmetric ratio (I_{02}/I_{01}) increases as vanadium content increases resulting in more colour purity in vanadate compounds bacause of more polarizing environment.Judd-ofelt analysis also shows that more polarising environment in phosphovanadate and vanadate compounds in comparison to phosphate. Lifetime measurement and quantum yield shows that phosphovanadate has longest lifetime and highest quantum yield among pure phosphate, phosphovanadate and vanadate host and this is due to more assymmetry around Eu^{3+} in phosphovanadate compared to vanadate and phosphate and more efficient energy transfer from vanadate to Eu^{3+}. Hence, the interplay of polarization and assymetry around $Eu^{3+}$are giving rise to desired photoluminescent properties in $KSrLa_{1-y}(PO_4)_x(VO4)_{2-x}$: yEu^{3+} system. Concentration quenching experiment clearly shows that FRET mechanism is responsible for quenching of Eu^{3+} luminescence in phosphovanadate host.

References:

1. (a) S. V. Eliseevaa and J. G. Bünzli, Chem. Soc. Rev., 2010, **39**, 189 (b) D. N. Woodruff, R. E. P. Winpenny and R. A. Layfie, Chem. Rev., 2013, **113**, 5110 (c) M. V. DaCosta, S. Doughan, Y. Han and U. J. Krull, Anal. Chim. Acta, 2014, **832**, 1 (d) J.G. Bunzli and C. Piguet, Chem. Soc. Rev., 2005, **34**, 1048.
2. Y. Tian, X. Qi, X. Wu, R. Hua and Baoji, J. Phys. Chem. C, 2009, **113**, 10767.
3. (a) M. Guzik , E. Tomaszewicz , Y. Guyot , J. Legendziewicz and G. Boulon, J. Mater. Chem. C, 2015, DOI: 10.1039/C5TC01109D (b) G. Jia , P. A. Tanner, C. Duan and J. Dexpert-G, J. Phys. Chem. C, 2010, **114**, 2769 (c) F. A. Rabuffetti , S. P. Culver , J. S. Lee and R. L. Brutchey, Nanoscale, 2014, **6**, 2909 (d) O. Lehmann , K. Kömpe and M. Haase, J. Am. Chem. Soc., 2004, **126**, 14935.
4. C.X. Qin, Y.L.Huang, L.Shi, G.Q.Chen, X.B.Qiao and H.J.Seo, J. Phys. D: Appl. Phys., 2009, **42**, 185105.

5. L.H. Yi, L.Y.Zhou, F.Z.Gong, Y.W.Lan, Z.F.Tong and J.H.Sun, Mater.Sci.Eng.B, 2010, **172**, 132.
6. (a) L. Li, Y. Su and G. Li, J. Mater. Chem., 2010, **20**, 459 (b) R. Yang, J. Qin, M. Li, Y. Liu and Fei L, CrystEngComm., 2011, **13**, 7284 (c) L. Zhang, M. Yin, H. You, M. Yang , Y. Song and Y. Huang, Inorg. Chem., 2011, **50**, 10608.
7. S. Xin, Y. Wang, Z. Wang, F. Zhang, Y .Wen, and G. Zhu; Electrochem. Solid-State Lett., 2011, **14**, H438.
8. X. Doua, W. Zhaoa, E. Songa, G. Zhoua, C. Yib and M. Zhoub, Spectrochim. Acta Part A, 2011, **78**, 821.
9. C. Zhang, H. Liang, S. Zhang, C. Liu, D. Hou, L. Zhou and G. Zhang, J. Phys. Chem. C, 2012, **116**, 15932.
10. X. Zhanga, L. Zhoua and M. Gongb, Optical Materials, 2013, **35**, 993.
11. C. Qin, Y. Huang and H. Jin Seo, J. Am. Ceram. Soc., 2013, 96, 1181.
12. S. Caoa, Y. Maa, C. Quanb, W. Zhua, K. Yanga, W. Yina, G. Zhenga, M. Wua and Z. Suna, J. Alloys Compd., 2009, **487**, 346.
13. Z. Tao, T. Tsuboi, Y. Huang, W. Huang, P. Cai and H. J. Seo, Inorg. Chem., 2014, **53**, 4161.
14. (a) A. A. Ansari, M. Alam, J. P. Labis, S. A. Alrokayan, G. Shafi, T. N. Hasan, N. A. Syed and A. A. Alshatwib, J. Mater. Chem., 2011, **21**, 19310 (b) T. V. Gavrilović, D. J. Jovanović, V. Lojpur and M. D. Dramićan, Scientific Reports, 2014, 4209 (c) Y. Zhang, H. He, W. Zhua and A. Zhenga, CrystEngComm., 2011, **13**, 6471.
15. H. Lin, Y. Fang, X. Huang and S. Chu; J. Am. Ceram. Soc., 2010, **93,** 138.
16. Y. Chang, C. Liang, S. Yan and Y. Shin, J. Phys. Chem. C, 2010, **114**, 3645 (b) Z. Zhou, N. Wang, N. Zhou, Z. He, Suqin Liu, Y. Liu, Z. Tian, Z. Mao and H. T. Hintzen, J. Phys. D: Appl. Phys., 2013, **46**, 035104
17. X. Zhou and X. Wang, Russ. J. Phys. Chem., 2013, **87,** 1859.
18. Z. Hou, P. Yang, C. Li, L. Wang, H. Lian, Z. Quan and J. Lin, Chem. Mater., 2008, **20**, 6686.
19. H. Ji, Z. Huang, Z. Xia, M. S. Molokeev, V. V. Atuchin and S. Huang, Inorg. Chem., 2014, **53**, 11119.
20. X. Hea, M. Guana, N. Liana, J. Suna and T. Shanga, J. Alloys Compd., 2010, **492**, 452.
21. Y. Zhang, G. Li, D. Geng, M. Shang and C. Peng, Inorg. Chem., 2012, **51**, 11655.

22. J. Rodriguez-Carvajal, Fullprof 2000 version 1.6, Laboratoire Leon Brillouin, Gif sur Yvette, France, 2000
23. K. Sugiyama and M. Tokonami, Mineral. J., 1990, **15**, 141.
24. J.C. Batista, P.C.D.S. Filho, O.A. Serra, *Dalton Trans*., 2012, **41**, 6310.
25. R. Phatak, S. K. Gupta, K. Krishnan, S. K. Sali, S.V.Godbole and A. Das, *Dalton Trans*., 2014, **43,** 3306.
26. L. Li, S. Zhang, *J. Phys. Chem. B*, 2006, **110**, 21438.
27. K. Binnemans, *Coord. Chem. Rev*., 2015, **295**, 1.
28. X.Y. Chen and G.K.J. Liu, *J. Solid State Chem*., 2005, **178,** 419.
29. C.C. Wu, K.B. Chen, C.S. Lee, T.M. Chen and B.M. Cheng, *Chem. Mater*., 2007, **19,** 3278.
30. K. Riwotzki and M. Hasse, *J. Phys. Chem. B*, 2001, **105,** 12709.
31. M. Keskar, Santosh K. Gupta, R. Phatak, S. Kannan and V. Natarajan, *J. Photochem. Photobiol. A*, 2015, **311,** 59.
32. S.K. Gupta, P.S. Ghosh, M. Sahu, K. Bhattacharyya, R. Tewari, V. Natarajan, *RSC Adv*., 2015, **5**, 58832.
33. G. Blasse, *J. Solid State. Chem*., 1986, **62,** 207.

Table of Content

In $KSrLa_{1-y}(PO_4)_x(VO_4)_{2-x}$: yEu^{3+} system, luminescence properties of Eu^{3+}can be enhanced via substitution of vanadate.